Egypt. J. Chem. **Vol. 67**, No. 7 pp. 171 - 182 (2024)

Egyptian Journal of Chemistry

http://ejchem.journals.ekb.eg/

Solvatochromic A-π_D-A Bithiophene Derivative, Steady State, Time Resolved Studies and DFT Calculations

Ahmed Soliman[a], Mohamed A. Ismail[b], Badr[a] A. El-Sayed, Ahmed Mora[a] and Ayman A. Abdel-Shafi[c]*

[a] *Chemistry Department, Faculty of Science, Al-Azhar University, Nasr City, Cairo, Egypt*
[b] *Department of Chemistry, Faculty of Science, Mansoura University, 35516 Mansoura, Egypt*
[c] Department of Chemistry, Faculty of Science, Ain Shams University, 11566, Abbassia, Cairo, Egypt

Abstract

Steady state and time resolved properties of 5-(5-(4-fluorophenyl)thiophen-2-yl)thiophene-2-carboxamidine (FTTA) in a variety of solvents are reported. FTTA presents system of the type A-p_D-A where the bithiophene bridge acts as electron donor and the 4-fluorophenyl and amidine groups at both terminals act as electron acceptors. Solvent effect on the absorption spectra shows a slight solvent polarity dependence that covers a narrow range from 368 nm in cyclohexane to 379 in acetonitrile. On the other hand, change of the fluorescence emission maximum in aprotic solvents was only about 40 nm from acetonitrile to cyclohexane. The larger variation of the fluorescence emission maximum with the polarity of the solvent gives a conjecture that the nature of emission of from a state with intramolecular charge transfer character. However, the small dependence of the absorption maximum on the solvent polarity is attributed to a smaller dipole moment of the ground state than that of the excited state. DFT calculations shows a planar geometry in the excited state and non-planar geometry in the ground state. Dipole moments obtained from DFT and TD-DFT are also reported. Fluorescence lifetime, t, and fluorescence quantum yield, F_f, were found to decrease with the emission energy, while the emission energy decreases as the solvent polarity increases. Furthermore, the Stokes shift has been found to increase as the solvent polarity increases. Stokes shift was also correlated with Reichardt's solvent polarity parameter, E_T^N from which the dipole moment change, Dm, was evaluated. To ascertain the contributions of specific and non-specific solute-solvent interactions, we have utilized multi-parametric relationships as developed by Kamlet-Taft, Catalán, and Laurence. In every instance, it was discovered that non-specific interactions were largely dominating.

Keywords: solvatochromism, Intramolecular charge transfer, linear solvation energy relationship, DFT calculations

1. Introduction

The investigation of the intramolecular charge transfer (ICT) phenomenon has received significant attention in recent years due to its diverse molecular structures [1-30]. Compounds known as push-pull systems, which feature an electron donating (D) group separated from an electron acceptor (A) group by a p-linker bridge in an organic D-π-A system, are a noteworthy class of molecules.The intramolecular charge transfer phenomenon (ICT) arises from the push-pull process. The ICT process is accountable for the polarization of the molecule and leads to a change in dipole moment upon electronic excitation. Push-pull compounds were widely used in nonlinear optical materials (NLO), solvatochromic probes [31-33], bioimaging [34], dye-sensitizing solar cells [35-37], and light-emitting diodes [38].

The Thiophene ring has been extensively incorporated in push-pull compounds, primarily serving as an electron donor or as a bridge. Carlotti et al.[5] conducted research on the impact of the thiophene ring as an electron-rich group on the spectral properties of push-pull compounds. Rasmussen et al. [6] also studied the photophysical properties of thiophene-based compounds. Some thiophene-based chromophores have been shown to

*Corresponding author e-mail: aaashafi@sci.asu.edu.eg.; (Ayman A. Abdel-Shafi).
EJCHEM use only: Received date 30 October 2023; revised date 06 December 2023; accepted date 07 January 2024
DOI: 10.21608/EJCHEM.2024.245680.8800

have a direct correlation between their spectral characteristics and the strength of the transitions' CT character, as demonstrated by Popczyk et al. [7] and predicted their hyperpolarizability [8]. Mencaroni et al. investigated the deactivation processes of excited states in one and two-armed push-pull systems with pyridine, furan, or thiophene as electron donors and nitro groups as electron acceptors in various solvents [9].

We have examined the fluorosolvatochromism of structurally similar compounds with different electron donating, bridge structure and electron withdrawing moieties [10-24]. We have recently analyzed the photophysical characteristics of cationic thiophene-based chromophores containing an electron-donating methoxy group and an electron-accepting amidine group, which ensure optimal performance. The dipole moment changes of both compounds, as determined experimentally, suggest emission from the ICT excited state and are consistent with the results from DFT calculations [22-24].

Effect of the π -bridge structure on the ICT processes were recently studied on 6-(5-(4-methoxyphenyl)furan-2-yl)nicotinonitrile and 4-(5-(4-methoxyphenyl)thiophen-2-yl)benzonitrilederivatives and found that the photophysical properties were largely influenced by the nature of the bridge structure. DFT calculations show that the geometry of 4-(5-(4-methoxyphenyl)thiophen-2-yl)benzonitrile is not planar in the ground state and planar in the excited state, while 6-(5-(4-methoxyphenyl)furan-2-yl)nicotinonitrile is planar in the ground and excited states [23, 24].

In this report, solvent effect on the photophysical properties of 5-(5-(4-fluorophenyl)thiophen-2-yl)thiophene-2-carboxamidine (FTTA) is examined. Correlation between the observed experimental changes in the photophysical properties with solvents of different polarity and hydrogen bonding interactions is investigated with different theoretical treatments. The studied compound belongs to A-π-A class of chromophores. Fluorescence lifetime measurements and steady state absorption and emission studies are to be examined in a variety of solvents. Influence of the polarity parameters on the photophysical properties are to be illustrated. In addition, the dipole moment in the ground and excited states are to be evaluated experimentally and theoretically. Participation of specific and non-specific interactions on the experimental and derived photophysical properties are to be examined. DFT and TD-DFT simulations were used to obtain geometry optimization and the dipole moments in the ground and excited states, respectively.

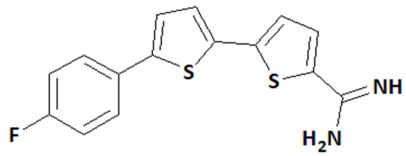

Scheme 1: Molecular structure of 5-(5-(4-fluorophenyl)thiophen-2-yl)thiophene-2-carboxamidine (FTTA)

2. Computational Studies and Geometry Optimization:

Geometry optimisation in the ground and excited states (DFT and DT-DFT) as well as calculations of the dipole moment were obtained using the Gaussian 09 software [39]. Cyclohexane, acetonitrile, and ethanol were the three solvents that were modelled using the B3LYP and 6-311+G(d,p) basis set. The B3LYP method is the most popular density-functional theory (DFT) approach due to its ability to accurately predict molecular structures and other properties. Fig. 1 shows the optimized geometry in both the ground and excited states, as well as the dipole moment vector. The phenyl ring containing the fluorine atom in chx has a twisted angle of 27.8°, and the phenyl ring containing the amidine group has a twisted angle of 18.0°, according to the ground state optimization. As can be seen in Fig. 1, the twisted angle of the terminal groups was discovered to be marginally smaller in acn and EtOH than in chx. The geometry of the excited state was found to be planar in all solvents in accordance with our previous findings [22-24].

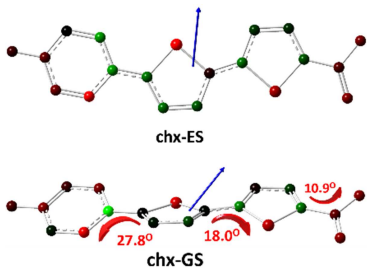

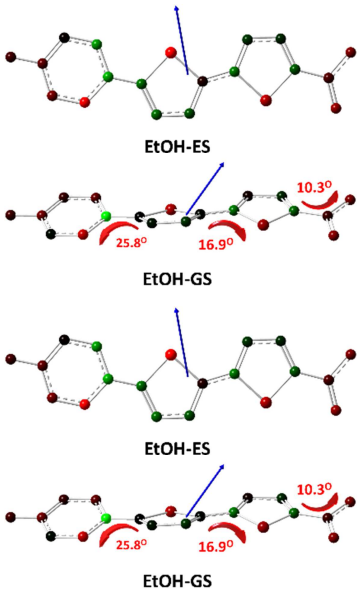

Fig. 1: The ground state and excited states geometry of FTTA in chx, acn, and EtOH, along with the dipole moment vector and charge distribution. In this illustration, the red and green colours represent the charge distributions

The positive and negative phases of the HOMO and LUMO frontier molecular orbitals for FTTC are displayed in Fig. 2, with the red and green regions, respectively representing these phases. Dipole moments obtained from DFT and TD-DFT calculations in acn, EtOH, and chx were determined to be 2.75 D, 3.59 D, and 3.56 D, in the ground state, m_g, and 3.96 D, 4.66 D, and 4.64 D in the excited states, m_e, respectively, which is close to the D-p-A previously reported systems [22-24].

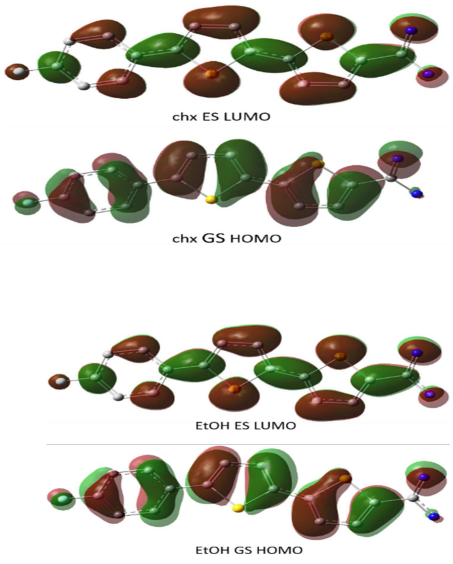

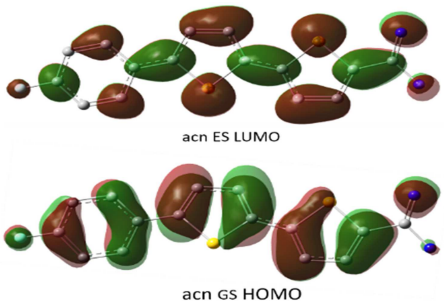

Fig. 2: The charge density distribution of HOMO and LUMO of FTTA obtained from TD-DFT simulations

3. Experimental

5-(5-(4-fluorophenyl)thiophen-2-yl)thiophene-2-carboxamidine (FTTA) was available from a previous studies and was fully characterized [30,31] and recrystallized twice from ethanol before use. Ethanol (EtOH), iso-butanol (iBuOH), n-butanol (nBuOH), 2-propanol (2PrOH), tetrahydrofurane (THF), dichloromethane (MC), acetonitrile (ACN), toluene (TOL), ethylacetate (EtAc), chloroform (CF), cyclohexane (CHX), 1,4-dioxane (DX), methanol (MeOH), were obtained from Sigma-Aldrich and used as received.

The UV-1900 UV-VIS Spectrophotometer from Shimadzu was used to collect the absorption spectra. The RF-6000 Spectrofluorophotometer was used to collect steady state fluorescence emission measurements. Fluorescence lifetimes were measured with Easylife from Optical Building Blocks, Canada (OBB) using a 375 nm LED as the excitation light source. Geometry optimisation in the ground and excited states (DFT and DT-DFT) as well as calculations of the dipole moment were obtained using the Gaussian 09 software [32]. Cyclohexane, acetonitrile, and ethanol were the three solvents that were modelled using the B3LYP and 6-311+G(d,p) basis set.

4. Results and Discussions

a) Steady State measurements

The absorption spectra in different solvents are shown in Fig. 3. It is clear from Fig. 3 that the absorption spectra are weakly sensitive to the solvent polarity and shows a small solvatochromism. FTTA shows a wavelength of maximum absorption of 380 nm and 376 nm in MC and chx, respectively. This can be attributed to a small dipole moment in the ground state. In neutral aqueous solution, the

wavelength of maximum absorption is 376 which does not correlate to the polarity parameter, which might be due to strong hydrogen bonding interactions. The fluorescence emission spectra in Fig. 4 were more prominent and displayed a more significant shift towards the red region compared to the absorption spectra in each solvent because of a larger dipole moment in the excited state due to the intramolecular charge transfer process upon electronic excitation.

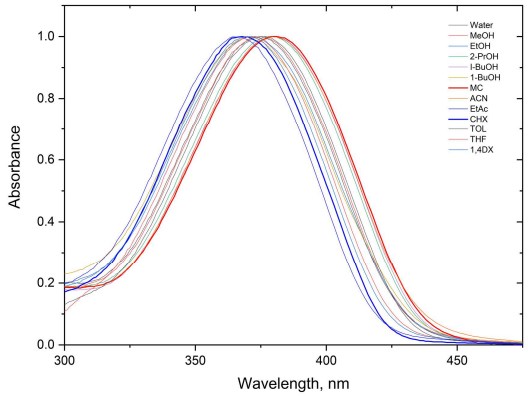

Fig. 3: Normalized absorption spectra of 5mM FTTC in different solvents

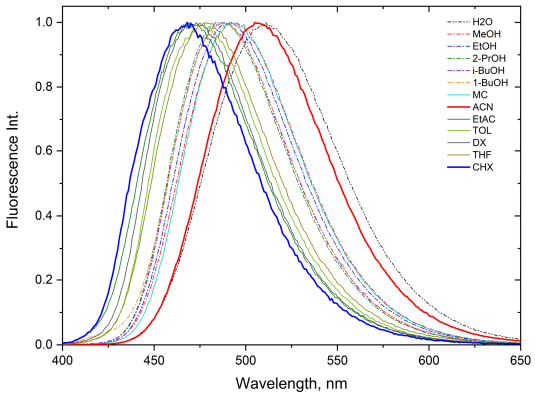

Fig. 4: Normalized fluorescence emission spectra of 5 mM FTTC in different solvents

Table 1 shows a small change in the maximum absorption wavenumber and considerable change in the maximum fluorescence emission wavenumber. In protic solvents, the average absorption energy is about 27027.3 ± 400 cm^{-1} and the average fluorescence emission wavenumber is 20460.0 ± 200 cm^{-1}. In general, the dependence of the maximum absorption wavenumber, ν_{abs}, on the solvent's dielectric constant, ε, is scattered while the dependence of the maximum emission wavenumber, ν_{em}, decreases as the solvent's dielectric constant, ε, increases as shown in Fig. 5 indicating stabilization of the excited intramolecular charge transfer state in polar solvents. This can be assigned to the higher charge transfer nature of the excited state.

Table 1: Photophysical properties of FTTA in different solvents

	Solvent	λ_a^{max}	λ_f^{max}	τ, ns	Φ_f	$k_r/10^8$ s^{-1}	$k_{nr}/10^8$ s^{-1}
1	Water	375	511	2.97	0.86	2.90	0.47
2	Methanol	374	494	2.39	0.89	3.72	0.46
3	Ethanol	371	490	2.31	0.97	4.20	0.13
4	2-Propanol	379	486	2.2	0.92	4.18	0.36
5	Iso-butanol	380	486	2.22	0.84	3.78	0.72
6	1-Buthanol	370	488	2.23	0.69	3.09	1.39
7	Methylene chloride	380	492	2.04	0.96	4.71	0.20
8	Acetonitrile	379	507	2.48	0.9	3.63	0.40
9	Tetrahydrofuran	372	478	1.41	0.71	5.04	2.06
10	1,4-Dioxane	370	473	1.1	0.6	5.45	3.64
11	Ethylacetate	366	471	1.08	0.38	3.52	5.74
12	Toluene	376	477	1.31	0.68	5.19	2.44
13	Cyclohexane	368	467	0.92	0.3	3.26	7.61

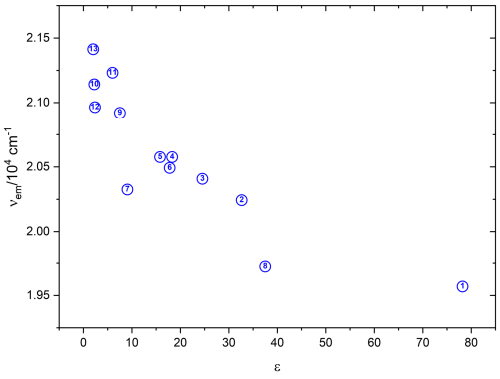

Fig. 5: The relationship between the emission energy, ν_{em}, and the dielectric constant of the solvent, ε.

The Stokes shift (the difference between absorption and emission energies) tends to increase as the dielectric constant (ε) increases, as demonstrated in Fig. 6 as a result of the decrease of the emission energy and approximately constant absorption energy. The decrease of the emission energy shown in Fig. 5 and increase of the Stokes shift shown in Fig. 6 with the solvent's dielectric constant, ε, is consistent with the intramolecular charge transfer nature of excited state.

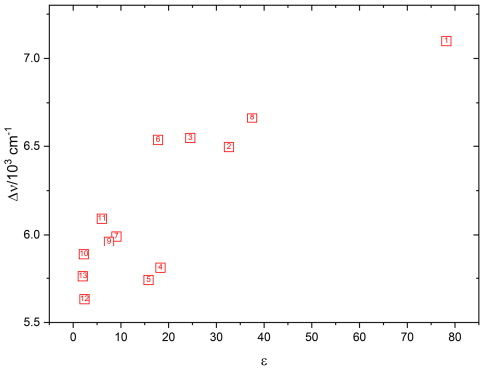

Fig. 6: The relationship between the Stokes shift, Δν, and the dielectric constants of the solvent, ε.

The fluorescence quantum yield was determined in various solvents by Eq. (1) as follows:

$$\Phi_u = \left(\frac{F_u}{A_u}\right)\left(\frac{A_s}{F_s}\right)\left(\frac{n_u^2}{n_s^2}\right)\Phi_s \qquad (1)$$

where A represents absorbance, n is the refractive index of the solvent, F is the integrated area of the fluorescence emission spectrum, while the subscripts u and s stand for the sample and the standard (1N H_2SO_4 (0.54)), respectively [42]. The obtained fluorescence quantum yields of FTTA in different solvents are collected in Tables 1. The fluorescence quantum yield decreases as the emission energy decreases, as presented in Fig. 7 which is consistent with the energy gap low [43], due to the higher radiationless deactivation processes as the energy gap between the excited and ground states decreases. It is also interesting to find out that the fluorescence quantum yield deviates in DMSO and DMF which can be attributed to the interaction of the amidine group with S=O of DMSO and C=O of DMF. One of the intriguing observations of FTTA is the high quantum yield in aqueous solution and relatively high quantum yield in protic solvents which indicate that hydrogen bonding interactions minimizes the non-radiative deactivation pathways (Table 1).

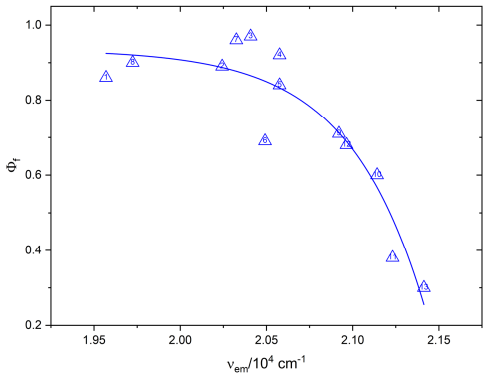

Fig. 7: The relationship between the fluorescence quantum yield and the emission energy, νem.

Fluorescence decay traces were found to fit with mono-exponential function as follows:

$$I(t) = a \ \ exp\left(\frac{-t}{\tau}\right) \qquad (2)$$

where I is the fluorescence intensity at time (t), a is the preexponential value, and τ is the fluorescence lifetime. The results of the fluorescence decay across the entire spectrum of fluorescence emission are shown in Tables 1. Fig. 8 shows that the fluorescence lifetime of FTTA decreases with the emission energy, ν_{em}, and Fig. 9 implies that the fluorescence lifetime increases as the solvent's polarity increases due to the stabilization of the excited ICT state. In other words, the fluorescence lifetime is higher in polar solvents than in non-polar solvents and inversely proportional to the emission energy, ν_{em}, in accordance with the energy gap low and higher radiationless deactivation as the emission energy decreases.

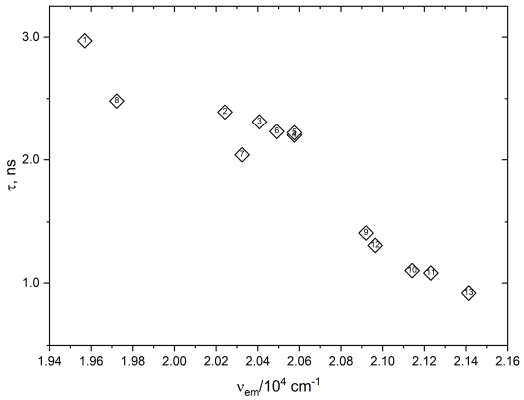

Fig. 8: Dependence of the fluorescence lifetime on the emission energy, ν_{em}, in different solvents.

Radiative ($k_r = \Phi_f/\tau$) and non-radiative ($k_{nr} = (1-\Phi_f)/\tau$) rate constants were collected in Table 1 and were found to decrease as the solvent polarity increases as shown in Fig. 10. It is clear from Fig. 10 that the dependence of the k_{nr} is more sensitive than k_r on the solvent's polarity. It is also important to correlate these findings with the decrease of the emission energy with the solvent polarity given in Fig. 5. Both observations lead to the expected increase in the radiationless rate constant as the emission energy decreases.

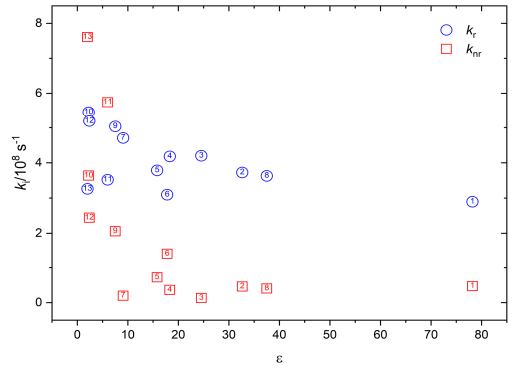

Fig. 10: Correlation of the radiative (*k*r) and non-radiative (*k*nr) rate constants with the dielectric constant of the solvent, ε.

The direction of the dipole moment vector obtained from the DFT calculations in both the ground and excited states (as shown in Fig. 1) indicates that the vector directions are not parallel in either state. Combination of the absorption and emission energies as given by as given by Bilot and Kawski ($\Delta\nu = \nu_a - \nu_e$) and ($\Sigma\nu = \nu_a + \nu_e$)) with the solvent parameters, $f(\varepsilon,n)$ and $\phi(\varepsilon,n)$, was found to be scattered [44-46].

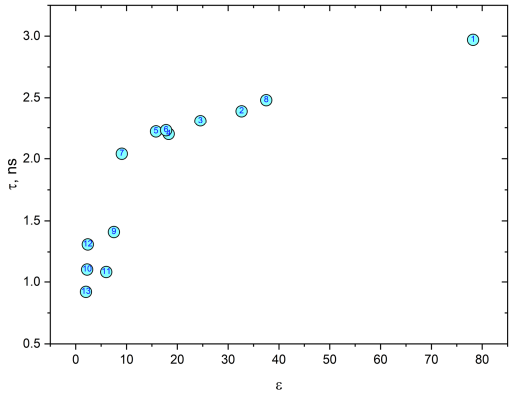

Fig. 9: Fluorescence lifetime, τ, dependence on the dielectric constant of the solvent, ε.

The correlation between the Stokes shift, Δν, and the solvent polarity parameter, E_T^N, as introduced by Reichardt [47] and further developed by Ravi [48], only shows a good correlation when the solvents are divided into two groups, as shown in Fig. 11. The dipole moment change, Δμ, can be evaluated from Eq. 4 using the slope of Eq. 3:

$$\Delta\nu = 11{,}307.6\left(\frac{\Delta\mu^2 a_B^3}{\Delta\mu_B^2 a^3}\right) E_T^N + \text{constant} \qquad (3)$$

$$\Delta\mu = \mu_e - \mu_g = \sqrt{\frac{81\ S}{11{,}307.6\left[\frac{6.2}{a}\right]^3}} \qquad (4)$$

where Δμ is the dipole moment change and a is the Onsager cavity radius for the reference betaine dye (B) and the FTTA. The obtained results of the Eq. 3 are as follows:

$\Delta\nu_p = 4361.5\ (\pm 450.0) + 2811.5\ (\pm 620.0)\ E_T^N$,
$R^2 = 0.87$ protic solvents (5)

$\Delta\nu_{ap} = 5524.0\ (\pm 135.0) + 2474.5\ (\pm 455.0)\ E_T^N$,
$R^2 = 0.81$ aprotic solvents (6)

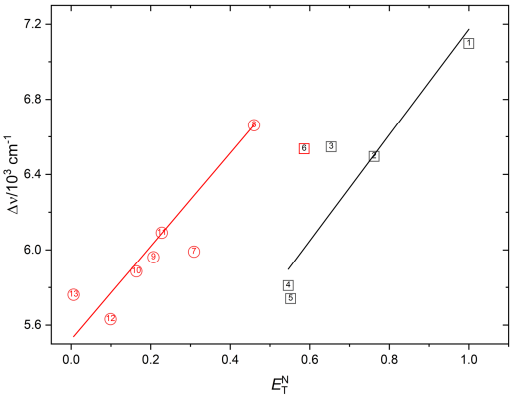

Fig. 11: Correlation of the Stokes shift with E_T^N parameter

The dipole moment changes, Δμ, were calculated using the slopes obtained from Eqs. 5 and 6 for $(\Delta\mu_e)_p$ = 4.3 D and $(\Delta\mu_e)_{ap}$ = 4.01 D in protic and aprotic solvents, respectively. The results were compared with the DFT calculations, and it was found that the dipole moment change, Δμ, obtained from Reichardt and Ravi [47, 48] was greater than the calculated value.

The clear illustration in Figure 11 of the data clustering unequivocally shows the importance of hydrogen bonding involvement in the photophysical properties of FTTA. Several relationships have been established to explain exactly how much solvent parameters, such as dipolarity/polarizability and hydrogen bonding interactions, contribute to the FTTA's photophysics.

where the polarizability (SP), dipolarity (SdP), acidity (SA), and basicity (SB) of the solvent are represented by the regression coefficients s, d, a, and b, respectively.

In a related study, Laurence et al. [53] developed a four-parameter regression equation to describe electrostatic (ES) and induction (DI) interactions, which included new parameters in addition to the previously determined specific interaction parameters.

Kamlet-Taft three parametric relationship [49, 50] which was early introduced the solvent dipolarity/polarizability, π*, the strength of solvent's hydrogen bond donation, α, and the strength of the solvent to receive protons, β, as follows.

$$A = A_0 + p\pi^* + a\alpha + b\beta \quad (7)$$

the susceptibility constants p, a and b represent the contribution of each item of the relationship. The solvent dependent property is represented by A, while that in the reference solvent is represented by A0.

Catalán's recently developed model [51, 52] involves splitting the Kamlet-Taft dipolarity/polarizability parameter (π*) into two parameters, solvent polarizability (SP) and dipolarity (SdP), as shown below:

$$A = A_0 + sSP + dSdP + aSA + bSB \quad (8)$$

$$A = A_0 + diDI + eES + a_1\alpha + b_1\beta \quad (9)$$

where α is solvent's acidity, β, and the solvent's basicity, β, while *di*, *e*, a_1, and b_1 are the regression coefficients.

Table 2 summarizes the findings of the multilinear regression analysis of Eqs. 7-9 and displays the relative contributions of each parameter to the photophysical property.

Table 2: Values acquired for the susceptibility constants according to Equations 7-9, based on the Kamlet-Taft, Catalán, and Laurence, relationships

		Kamlet				Catalan				Laurence		
n_{abs}	A_0	27203.7±(187.2)	%	R^2	A_0	31367.0±(958.3)	%	R^2	A_0	32433.9±(1117.0)	%	R^2
	p	-993.1±(236.5)	33.3	0.87	*s*	-5666.8±(1310.5)	74.1	0.87	*di*	-6448.9±(1403.3)	71.5	0.89
	a	964.0±(180.3)	32.3		*d*	-1346.8±(293.0)	17.6		*e*	-2058.9±(330.9)	22.8	
	b	-1028.8±(265.6)	34.5		*a*	360.9±(308.2)	4.7		a_1	84.6±(205.8)	0.9	
					b	274.1±(327.0)	3.6		b_1	427.4±(348.2)	4.7	
n_{em}	A_0	22369.2±(143.5)			A_0	22005.3±(779.0)			A_0	21099.4±(1146.3)		
	p	-1838.0±(192.3)	60.9	0.95	*s*	372.4±(1072.2)	11.0	0.95	*di*	1198.1±(1440.1)	23.9	0.93
	a	-575.8±(129.9)	19.1		*d*	-2419.5±(250.3)	71.7		*e*	-2815.7±(343.2)	56.2	
	b	-606.3±(210.3)	20.1		*a*	-284.6±(249.1)	8.4		a_1	15.3±(207.4)	0.3	
					b	299.6±(235.0)	8.9		b_1	977.2±(351.9)	19.5	
Dn	A_0	5445.8±(192.8)			A_0	5790.4±(786.2)			A_0	5944.6±(914.0)		
	p	738.4±(277.6)	42.4	0.79	*s*	-416.7±(1075.2)	20.0	0.86	*di*	-551.4±(1148.6)	28.1	0.89
	a	420.2±(175.1)	24.1		*d*	954.6±(240.3)	45.7		*e*	1093.5±(274.0)	55.7	
	b	581.4±(307.9)	33.4		*a*	547.6±(252.9)	26.2		a_1	248.5±(167.0)	12.7	
					b	169.2±(268.3)	8.1		b_1	70.5±(295.3)	3.6	
t	A_0	0.67±(0.19)			A_0	1.31±(0.73)			A_0	-0.29±(0.83)		
	p	1.19±(0.25)	50.14	0.88	*s*	-0.65±(0.98)	23.16	0.93	*di*	1.44±(1.04)	30.09	0.95
	a	0.81±(0.17)	34.09		*d*	1.49±(0.21)	53.51		*e*	2.07±(0.25)	43.22	
	b	0.37±(0.28)	15.76		*a*	0.60±(0.23)	21.35		a_1	0.53±(0.15)	11.14	
					b	-0.06±(0.21)	1.98		b_1	-0.74±(0.25)	15.54	
F_f	A_0	0.35±(0.10)			A_0	1.62±(0.45)			A_0	1.50±(0.64)		
	p	0.65±(0.17)	36.23	0.78	*s*	-1.80±(0.63)	76.12	0.80	*di*	-0.89±(0.78)	53.45	0.70
	a	0.66±(0.13)	36.87		*d*	0.35±(0.14)	14.94		*e*	0.15±(0.18)	8.84	
	b	-0.48±(0.18)	26.91		*a*	0.07±(0.14)	3.12		a_1	0.19±(0.14)	11.64	
					b	0.14±(0.14)	5.82		b_1	-0.43±(0.18)	26.07	

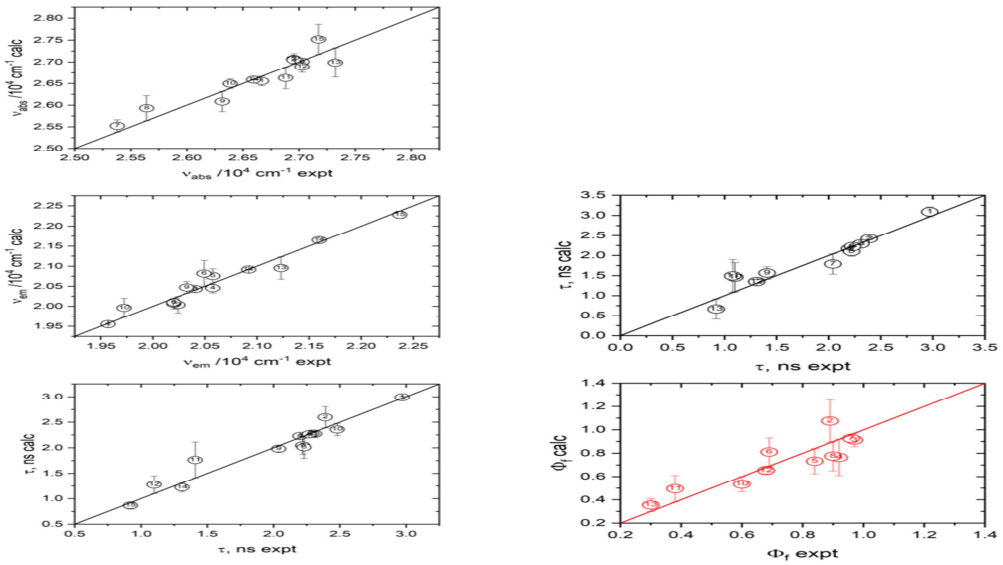

Fig. 12: The calculated photophysical properties, ν_{abs}, ν_{em}, $\Delta\nu$, Φ_f and τ, versus the corresponding experimental data using the Kamlet-Taft model Eq. 7.

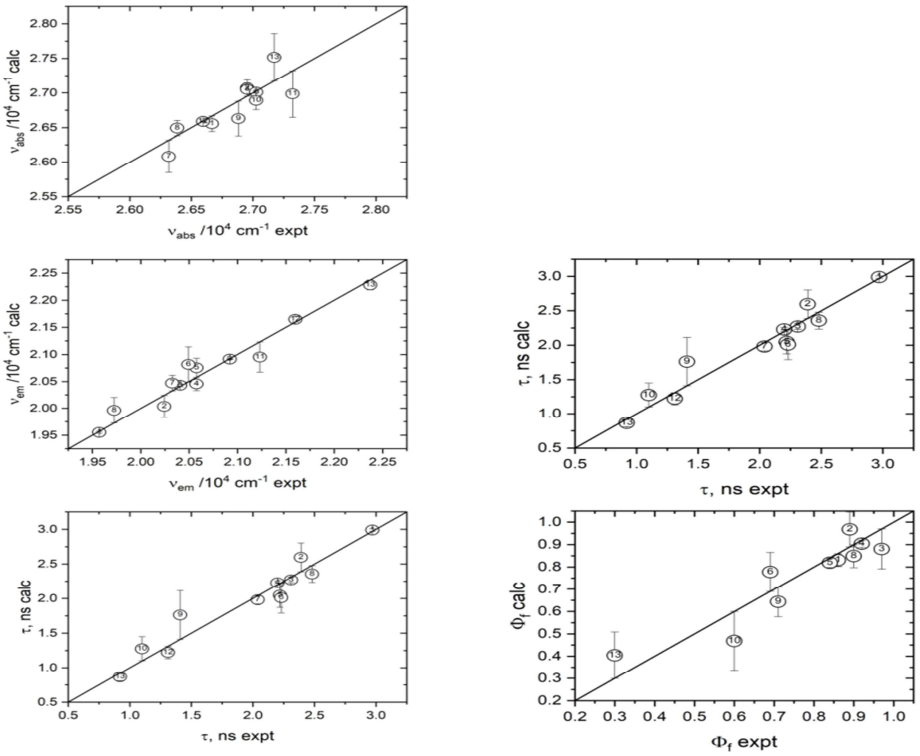

Fig. 13: The calculated photophysical properties, ν_{abs}, ν_{em}, $\Delta\nu$, Φ_f and τ, versus the corresponding experimental data using Catalán's model Eq. 8.

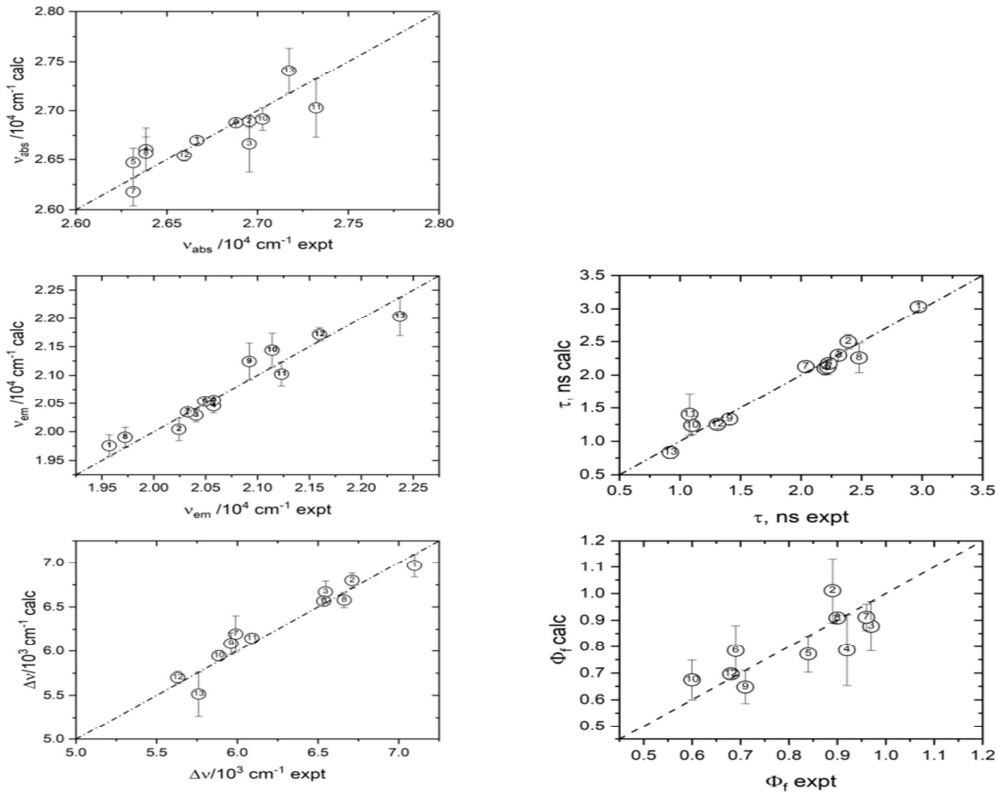

Fig. 14: The calculated photophysical properties, ν_{abs}, ν_{em}, $\Delta\nu$, Φ_f and τ, versus the corresponding experimental data using Laurence's model Eq. 9.

Table 2 illustrates the impact of each parameter on the photophysical property. The utilization of the three models on the absorption energy discloses that the contribution of non-specific interactions as estimated by Kamlet-Taft is only 33.3%, whereas the contribution given by Catalan or Laurence is approximately 90.0%. Such large contribution of the non-specific interactions indicates the weak dependence of the absorption energy on the hydrogen bonding interactions. On the other hand, the contribution of the non-specific interactions on the emission energy is the major contribution as given by the three models with percentage contribution of about 61.0%, 86.0% and 80.0 % by Kamlet-Taft, Catalán and Laurence, respectively. The Dependence of the Stokes shift on the solvent parameters given by the three models shows that the contribution of the nonspecific interactions is about 42.0%, 66.0% and 84.0 % as given by Kamlet-Taft, Catalán and Laurence, respectively. The dependence of the lifetime on the solvent parameters shows that the contribution of non-specific interactions of about 50.0 % by Kamlet-Taft and about 75.0% by Catalán or Laurence. The dependence of the fluorescence quantum yield on the solvent parameters is not the same by the three models as it is about 36.0 by Kamlet-Taft, 91.0 % by Catalan and 62.0 % by Laurence. Despite the fact that the contributions of the specific and non-specific interactions given by the three models are not similar, the higher contribution of the non-specific interactions is consistent with the intramolecular charge transfer process in the ground and excited states.

5. Conclusion

The photophysical properties of A-π-A system were studied in different solvents using steady-state and time-resolved measurements. Steady state measurements show a clear weak dependence of the ground state absorption on the nature of the solvent, while the effect of solvent on the steady state fluorescence emission spectra was much pronounced. However, the observed bathochromic shift with

solvent nature was much weaker than the previously reported D-p-A systems [43] due to the lower values of the excited state dipole moments of the former system. It has also been found that the fluorescence lifetime, τ, correlates very well with the excited state energy and solvent's polarity, in accordance with the ICT nature of the excited state. The relationship between the photophysical properties and the solvent polarity parameter, E_T^N, highlighted the importance of hydrogen bonding interactions.

The multilinear regression analysis with four parameters, developed by Catalán and Laurence et al., was employed to assess the influence of each solvent parameter on the photophysical properties. It has been found that while non-specific interactions are dominating, while specific interactions have a significant impact. Results of both models show that non-specific interactions tend to dominate, yet specific interactions have a noteworthy influence.

6. References

[1] F. Bureš, Fundamental aspects of property tuning in push–pull molecules, RSC Adv. 4(102) (2014) 58826-58851.

[2] N. Friebe, K. Schreiter, J. Kübel, B. Dietzek, N. Moszner, P. Burtscher, A. Oehlke, S. Spange, Fluorosolvatochromism of furanyl-and thiophenyl-substituted acetophenones, New J. Chem. 39(7) (2015) 5171-5179.

[3] M.K. Sadigh, M. Zakerhamidi, A. Shamkhali, Contribution of environment polarity effects on the nonlinear hyperpolarizability and linear optical characteristics of some phenothiazines, J. Mol. Liq. 336 (2021) 116328.

[4] Y. Rout, C. Montanari, E. Pasciucco, R. Misra, B. Carlotti, Tuning the fluorescence and the intramolecular charge transfer of phenothiazine dipolar and quadrupolar derivatives by oxygen functionalization, J. Am. Chem. Soc. 143(26) (2021) 9933-9943.

[5] B. Carlotti, A. Cesaretti, G. Cacioppa, F. Elisei, I. Odak, I. Škorić, A. Spalletti, Fluorosolvatochromism and hyperpolarizability of one-arm and two-arms nitro-compounds bearing heterocyclic rings, J. Photochem. Photobiol. A: Chem. 368 (2019) 190-199.

[6] S.C. Rasmussen, S.J. Evenson, C.B. McCausland, Fluorescent thiophene-based materials and their outlook for emissive applications, Chem. Commun. 51(22) (2015) 4528-4543; and references therein.

[7] A. Popczyk, Y. Cheret, A. Grabarz, P. Hanczyc, P. Fita, A. El-Ghayoury, L. Sznitko, J. Mysliwiec, B. Sahraoui, Tunable photophysical properties of thiophene based chromophores: A conjoined experimental and theoretical investigation, New J. Chem. 43(17) (2019) 6728-6736.

[8] A. Popczyk, Y. Cheret, A. El-Ghayoury, B. Sahraoui, J. Mysliwiec, Solvatochromic fluorophores based on thiophene derivatives for highly-precise water, alcohols and dangerous ions detection, Dyes Pigm. 177 (2020) 108300.

[9] L. Mencaroni, B. Carlotti, A. Cesaretti, F. Elisei, A. Grgičević, I. Škorić, A. Spalletti, Competition between fluorescence and triplet production ruled by nitro groups in one-arm and two-arm styrylbenzene heteroanalogues, Photochem. Photobiol. Sci. 19(12) (2020) 1665-1676.

[10] A.M. Dappour, M.A. Taha, M.A. Ismail, A.A. Abdel-Shafi, Solvatochromic behavior of D-π-A bithiophene carbonitrile derivatives, J. Mol. Liq. 286 (2019) 110856.

[11] M.A. Taha, A.M. Dappour, M.A. Ismail, A.H. Kamel, A.A. Abdel-Shafi, Solvent polarity indicators based on bithiophene carboxamidine hydrochloride salt derivatives, J. Photochem. Photobiol., A 404 (2021) 112933.

[12] A.A. Abdel-Shafi, M.A. Ismail, S.S. Al-Shihry, Effect of solvent and encapsulation in β-cyclodextrin on the photophysical properties of 4-[5-(thiophen-2-yl) furan-2-yl] benzamidine, J. Photochem. Photobiol., A 316 (2016) 52-61.

[13] A.S. Amer, A.M. Alazaly, A.A. Abdel-Shafi, Solvatochromism of 1-naphthol-4-sulfonate photoacid and its encapsulation in cyclodextrin derivatives, J. Photochem. Photobiol., A 369 (2019) 202-211.

[14] A.M. Alazaly, A.S. Amer, A.M. Fathi, A.A. Abdel-Shafi, Photoacids as singlet oxygen photosensitizers: Direct determination of the excited state acidity by time-resolved spectroscopy, J. Photochem. Photobiol., A 364 (2018) 819-825.

[15] A.A. Abdel-Shafi, S.S. Al-Shihry, Fluorescence enhancement of 1-napthol-5-sulfonate by forming inclusion complex with β-cyclodextrin in aqueous solution, Spectrochim. Acta A Mol. Biomol. Spectrosc. 72(3) (2009) 533-537.

[16] A.A. Abdel-Shafi, Effect of β-cyclodextrin on the excited state proton transfer in 1-naphthol-2-sulfonate, Spectrochim. Acta A Mol. Biomol. Spectrosc. 57(9) (2001) 1819-1828.

[17] M.A. Abdelzaher, Performance and hydration characteristic of dark white evolution (DWE) cement composites blended with clay brick powder, Egypt. J. Chem. 65(8) (2022) 419-427.

[18] M.A. Abdelzaher, A.S. Hamouda, I.M. Ismail, M. El-Sheikh, Nano titania reinforced limestone cement: physico-mechanical investgation, Key Eng. Mater. 786 (2018) 248-257.

[19] H.N. Akl, A.M. Alazaly, D. Salah, H.S. Abdel-Samad, A.A. Abdel-Shafi, Effects on the photophysical properties of naphthylamine derivatives upon their inclusion in cyclodextrin nanocavities, J. Mol. Liq. 311 (2020) 113319.

[20] A.A. Abdel-Shafi, Inclusion complex of 2-naphthylamine-6-sulfonate with β-cyclodextrin: Intramolecular charge transfer versus hydrogen bonding effects, Spectrochim. Acta A Mol. Biomol. Spectrosc. 66(4-5) (2007) 1228-1236.

[21] H.A. Sabek, A.M. Alazaly, D. Salah, H.S. Abdel-Samad, M.A. Ismail, A.A. Abdel-Shafi,

Photophysical properties and fluorosolvatochromism of D–π–A thiophene based derivatives, RSC Adv. 10(71) (2020) 43459-43471.
[22] M.M. Khaled, M.A. Ismail, H.A. Medien, A.A. Abdel-Shafi, H.S. Abdel-Samad, Photophysical properties of push-pull monocationic D-π-A+ thiophene based derivatives: Fluorosolvatochromism and pH studies, Spectrochim. Acta A Mol. Biomol. Spectrosc. 288 (2023) 122090.
[23] M. Shahin, A.M. Alazaly, M.A. Ismail, A.A. Abdel-Shafi, Effect of the π-bridge structure on the intramolecular charge transfer of push–pull 2-phenylthiophene and 2-(furan-2-yl) pyridine derivatives, J. Mol. Liq. 378 (2023) 121624.
[24] M.A.I. H. Mahmoud, H. A.A. Medien, H. S. Abdel-Samad, Ayman A. Abdel-Shafi, Unique structural effect on the fluorosolvatochromism and dual fluorescence emission of D-p-A+ cationic chromophores with furyl bridge. An approach to white light emitters, Spectrochim. Acta A: Mol. Biomol. Spectro. (in press.) (2024).
[25] S. Yang, C. Cao, J. Li, Z. Deng, S. Ni, J.-X. Jian, Q.-X. Tong, L. Dang, M.-D. Li, Unveiling the π-Chain Effect on Charge Transfer and Charge Recombination Among Donor– π–Acceptor Material Systems, J. Phys. Chem. C 126(2) (2022) 1076-1084.
[26] N.N.M.Y. Chan, A. Idris, Z.H.Z. Abidin, H.A. Tajuddin, Z. Abdullah, Intramolecular charge transfer-induced solvatochromism and large Stokes shifts of furocoumarins, Mat. Chem. Phys. 276 (2022) 125406.
[27] Z. Lou, P. Zhou, Theoretical exploration in the substituent effect on photophysical properties and excited-state intramolecular proton transfer process of benzo [a] imidazo [5, 1, 2-cd] indolizines, J. Photochem. Photobiol. A 422 (2022) 113570.
[28] H. Dai, H. Zeng, H. Li, J. Long, K.W. Ng, Y. Wang, B. Xu, G. Shi, Z. Chi, C. Liu, Manipulation of excited-state intramolecular proton transfer by electron-donor substitution for high performance fluoride ions sensing, Spectrochim. Acta A 306 (2024) 123530.
[29] C. Jih, C.-H. Chen, Role of π-bridge and strong solid-state emission in triphenylamine-benzothiazole based nonlinear optical dyes, J. Photochem. Photobiol. A 447 (2024) 115225.
[30] H. Mandal, J.L. Rao, J.i. Kulhánek, F. Bureš, P.R. Bangal, Understanding of Intramolecular Charge Transfer Dynamics of a Push–Pull Dimethylamino-phenylethynylphenyl-dicyanoimidazole by Steady-State and Ultrafast Spectroscopic Studies, J. Phys. Chem. C 127(9) (2023) 4724-4740.
[31] C. Reichardt, T. Welton, Solvents and solvent effects in organic chemistry, 4th ed., John Wiley & Sons2010.
[32] E.V. Verbitskiy, P. Le Poul, F. Bureš, S. Achelle, A. Barsella, Y.A. Kvashnin, G.L. Rusinov, V.N. Charushin, Push–Pull Derivatives Based on 2, 4′-Biphenylene Linker with Quinoxaline,[1, 2, 5] Oxadiazolo [3, 4-B] Pyrazine and [1, 2, 5] Thiadiazolo [3, 4-B] Pyrazine Electron Withdrawing Parts, Molecules 27(13) (2022) 4250.
[33] A.K. Kushwaha, Y. Kumar, S. Kumar, R.S. Singh, Competitive ICT in asymmetric D– A Scaffolds showing visible solvatochromism, temperature-induced emission enhancement and AIE based acidochromism, J. Lumin. 250 (2022) 119072.
[34] J. Shaya, P.R. Corridon, B. Al-Omari, A. Aoudi, A. Shunnar, M.I.H. Mohideen, A. Qurashi, B.Y. Michel, A. Burger, Design, photophysical properties, and applications of fluorene-based fluorophores in two-photon fluorescence bioimaging: A review, J. Photochem. Photobiol., C (2022) 100529.
[35] Y. Wu, W. Zhu, Organic sensitizers from D–π–A to D–A–π–A: effect of the internal electron-withdrawing units on molecular absorption, energy levels and photovoltaic performances, Chem. Soc. Rev. 42(5) (2013) 2039-2058.
[36] C. Duan, K. Zhang, C. Zhong, F. Huang, Y. Cao, Recent advances in water/alcohol-soluble π-conjugated materials: new materials and growing applications in solar cells, Chem. Soc. Rev. 42(23) (2013) 9071-9104.
[37] M. Liang, J. Chen, Arylamine organic dyes for dye-sensitized solar cells, Chem. Soc. Rev. 42(8) (2013) 3453-3488.
[38] Y. Ohmori, Development of organic light-emitting diodes for electro-optical integrated devices, Laser Photonics Rev. 4(2) (2010) 300-310.
[39] R.A. Gaussian09, 1, mj frisch, gw trucks, hb schlegel, ge scuseria, ma robb, jr cheeseman, g. Scalmani, v. Barone, b. Mennucci, ga petersson et al., gaussian, Inc., Wallingford CT 121 (2009) 150-166.
[40] M.A. Ismail, A. Negm, R.K. Arafa, E. Abdel-Latif, W.M. El-Sayed, Anticancer activity, dual prooxidant/antioxidant effect and apoptosis induction profile of new bichalcophene-5-carboxamidines, Eur. J. Med. Chem. 169 (2019) 76-88.
[41] M.A. Ismail, M.M. Youssef, R.K. Arafa, S.S. Al-Shihry, W.M. El-Sayed, Synthesis and antiproliferative activity of monocationic arylthiophene derivatives, Eur. J. Med. Chem. 126 (2017) 789-798.
[42] A.M. Brouwer, Standards for photoluminescence quantum yield measurements in solution (IUPAC Technical Report), Pure Appl. Chem. 83(12) (2011) 2213-2228 ; and references therein.
[43] N.J. Turro, V. Ramamurthy, V. Ramamurthy, J.C. Scaiano, Principles of molecular photochemistry: an introduction, University science books2009.
[44] L. Bilot, A. Kawski, Effect of the solvent on the electronic spectrum of luminescent molecules, Z. Naturforsch 18a (1963) 10-15.
[45] v.L. Bilot, A. Kawski, Zur theorie des einflusses von Lösungsmitteln auf die elektronenspektren der moleküle, Z. Naturforsch 17a (7) (1962) 621-627.
[46] A. Kawski, P. Bojarski, Comments on the determination of excited state dipole moment of molecules using the method of solvatochromism,

Spectrochim. Acta, Part A 82(1) (2011) 527-528; and references therein.
[47] C. Reichardt, Solvatochromic dyes as solvent polarity indicators, Chem. Rev. 94(8) (1994) 2319-2358.
[48] M. Ravi, T. Soujanya, A. Samanta, T. Radhakrishnan, Excited-state dipole moments of some Coumarin dyes from a solvatochromic method using the solvent polarity parameter, ENT, J. Chem. Soc., Faraday Trans. 91(17) (1995) 2739-2742.
[49] M.J. Kamlet, J.L.M. Abboud, M.H. Abraham, R. Taft, Linear solvation energy relationships. 23. A comprehensive collection of the solvatochromic parameters,. pi.*,. alpha., and. beta., and some methods for simplifying the generalized solvatochromic equation, J. Org. Chem. 48(17) (1983) 2877-2887.
[50] Y. Marcus, The properties of organic liquids that are relevant to their use as solvating solvents, Chem. Soc. Rev. 22(6) (1993) 409-416.
[51] J. Catalán, Toward a generalized treatment of the solvent effect based on four empirical scales: dipolarity (SdP, a new scale), polarizability (SP), acidity (SA), and basicity (SB) of the medium, J. Phys. Chem. B 113(17) (2009) 5951-5960.
[52] J. Del Valle, F. García Blanco, J. Catalán, Empirical parameters for solvent acidity, basicity, dipolarity, and polarizability of the ionic liquids [BMIM][BF4] and [BMIM][PF6], J. Phys. Chem. B 119(13) (2015) 4683-4692.
[53] C. Laurence, J. Legros, A. Chantzis, A. Planchat, D. Jacquemin, A database of dispersion-induction DI, electrostatic ES, and hydrogen bonding α1 and β1 solvent parameters and some applications to the multiparameter correlation analysis of solvent effects, J. Phys. Chem. B 119(7) (2015) 3174-3184.

.